Effect of the surface morphology over the fatigue performance of metallic single lap-shear joints

Effect of the surface morphology over the fatigue performance of metallic Single Lap-Shear Joints

F. Moroni[1], F. Musiari[1], C. Favi[1]

[1]Università degli Studi di Parma, Dipartimento di Ingegneria e Architettura, Parco Area delle Scienze, 181/A, 43124 Parma, IT.

Corresponding author: Francesco Musiari: francesco.musiari@unipr.it

The effect provided by the state of the surface on the quality of the adhesion, as well as the sensitivity of the position of the locus of failure to the surface morphology, is known to be one of the most crucial issue to be addressed when evaluating the capability of the bonded joint to withstand any mechanical stress . Therefore, the need for the substrates to undergo a pre-treatment before being bonded is to be considered. In this work, different pre-treatments were selected to be applied over aluminum and stainless steel adherents' surfaces with the goal to produce single lap joints to undergo cyclic loading until complete failure. In particular, the experimental campaign aimed to correlate the morphology generated by the different surface pre-treatment (laser ablation, grit blasting and simple degreasing) with the quality of the fatigue performance, measured as the number of cycles to failure. Result of this research shows that the surface morphology generated by the laser ablation was able to reduce or avoid interfacial failures, leading to an increase of the fatigue performances if compared with grit blasted and degreased joints.

Keywords: C. fatigue, B. Surface Treatment, B. Aluminum, B. Steel

1 Introduction

The wide diffusion of adhesively bonded joints which occurred in the last decades in many industrial fields did not simultaneously result in a similarly extensive employment of this technology for structural application. The main reason can be found in the poor confidence in the mechanical performance of the adhesively bonded joints, with particular refer to their usage in presence of critical environmental conditions or cyclic loading (or often the coexistence of both these disadvantageous conditions) [1]. Therefore, the capability to provide additional information on the behavior of the joints in a hot-humid exposure and subjected to a dynamic load became more and more relevant, especially considering the limits of the existing literature (few works with conflicting results) [2]. In particular, both the development of predictive tools able to estimate the lifetime of bonded joints and the performance of experimental characterization aiming at the identification of process parameters the affect the response of the joints in the aforementioned test conditions become crucial. The widest attempt to extend a fracture mechanics approach to the characterization of the crack growth in a cyclically loaded adhesively bonded joint was due to Mostovoy and Ripling [3]. The authors explored the trend of the crack growth rate on aluminium Tapered Double Cantilever Beam (TDCB) joints bonded with an epoxy resin, validating the use of the Paris' law for the central range of their experimental data. In addition, the authors identified the existence of a threshold strain energy release rate below which the crack growth rate was not detectable for this kind of joints. Countless works were dedicated to the study of the fatigue failure of Single Lap Joints (SLJs), which in general, regardless to the specimen geometry, is typically divided into two different phases [4][5]: (i) the crack initiation, which in SLJs typically occurs in correspondence of the corner singularities at the adherend terminations, and (ii) the subsequent crack propagation. Although many authors chose to focus the lifetime estimation only to the crack propagation stage, there are several works which took into account also the first phase of the failure. As instance, in a work by Imanaka *et al* [6] the strength and the lifetime associated to the crack initiation in a SLJ were estimated by means of the stress intensity factor and the order of stress singularity evaluated around the end of the overlap area. Shenoy *et al* [7] used the backface strain technique on aluminium/epoxy SLJs to divide the crack growth into steps and to find that low fatigue loads (lower than 50% of the quasi-static failure load) induce an initiation dominating failure in the joint. The same measurement method was used in several works by Zhang [8], Solana [9], Deng [10] and many others. Another technique frequently used for detecting the crack initiation and following the evolution of the crack path along the overlap length is the video microscopy. Although this method was strictly sensitive to the visibility conditions of the crack and it is based upon the main assumption that the crack initiates always at the edges of the joint in correspondence

of the overlap extremities, it can however provide useful information, taking care to observe both sides of the joint. Harris and Fay [11] analysed the fatigue life of adhesives for automotive applications and employed the video microscopy on one side of a SLJ to detect the crack initiation. Even Quaresimin and Ricotta [12] used visual inspection to evaluate the percentage of lifetime spent for the crack nucleation, finding that it may range from 20% to 70% depending from the overlap length and the load level, which pointed out the need to develop models able to take into account also the presence of this phase. However, the monitoring of the crack propagation remains the main field of employment of these methods and even others [13] [14] [15]. In this work, the focus is placed over the sensitivity of the fatigue behavior of adhesively bonded joints with metallic substrates to the pre-treatment used to prepare the surface aimed to be bonded. Indeed, it is well documented [16] how the state of the surface, from both a morphological and a chemical point of view, usually plays a significant role in determining the quality of the adhesion and, consequently, the mechanical strength of the joint. In [17] da Silva *et al* tested the influence of a series of scratches induced on the surface of some aluminium substrates of SLJs over the joint strength. Two different chemical pre-treaments were assessed (simple degreasing with acetone and chromic acid etching, respectively) and two different adhesives (brittle and ductile) were experimented. Results show how the grooves in the simply degreased surface had exhibited a strong influence on the static and fatigue strength of the joints when the failure on the specimens with no grooves was interfacial, which occurred when the brittle adhesive was employed and no chemical etching was applied. The surface morphology was primarily correlated to the roughness and consequently to the occurrence of the mechanical interlocking effect between surface and adhesive, even if the influence of this mechanism of adhesion is still topic of debate. Other works [18][19] pointed out a direct relation between the increase of the surface roughness and the corresponding increase of the mechanical strength of the joint and ascribed this phenomenon to the simultaneous effect of the mechanical interlocking and of the improvement of the load bearing area. On the same topic, few works [20][21] did not find any apparent correlation between the interfacial toughness of the joint and the surface roughness, but in many cases the detected increase of strength with the roughness was attributed not directly to the roughness. As instance, in [22] the random distribution of the asperities induced by a sandblasting treatment over aluminium and stainless steel butt joints was assumed to be capable to prevent the crack from propagating along a weak boundary interfacial layer. In [23] the increase of the peel strength in polyethylene/metal joints with the roughness was justified considering that the viscoelastic energy dissipation associated to the failure involved an higher volumetric amount of adhesive with respect to the smooth surface case. On the other hand, in [24] the lap shear strength of SLJs was recorded to be more sensitive to the features of the surface

asperities rather than to the macroscopic roughness. Moreover, it is worth noting that often the pre-treatments aimed at increasing the surface roughness can also induce changes on the chemical status of the surface itself, whose effect over the wettability was the main responsible of the corresponding increase of the mechanical strength [25]. In particular, the relation between the wettability and the surface roughness was found [26][27] to be increased with the roughness until a threshold after which becomes decreasing, because the asperities prevent the adhesive from spreading into the grooves. Consistently with this trend, even the adhesive fracture energy threshold of aluminium/epoxy joints was found to reach its lowest levels for both very high and very low values of surface roughness [28]. Therefore, with specific refer to the topic of this work, the possible correlation between the fatigue strength of the joints and the pre-treatments preliminarily applied over the substrates surfaces has to be investigated. Pereira [29] tested both an abrasive preparation and sodium dichromate-sulphuric acid etching over aluminium SLJs. Bland *et al* [30] took into account the coupled effect of a phosphoric acid anodizing and of the immersion in water over the fatigue response of aluminium tapered Double Cantilever Beam (DCB) joints, finding that the pre-treatment reached to ensure higher adhesive fracture energy with respect to the grit blasting. Even laser ablation arose in the last decades as a satisfactory pre-treatment for adhesive bonding purposes. The benefits brought to the joint strength were widely described in many works, dedicated both to the static characterization [31][32] and to the effect that the ablation has over the durability of the joints when exposed to a critical hot-humid environment [33][35]. However, the possible influence of the laser ablation over the fatigue response of joints was poorly touched by the existing literature. The authors in a previous work [35] performed an experimental campaign over a series of DCB specimens with the aim to compare the effect of the laser ablation over the fatigue response of the joints and, simultaneously, to investigate the different result attainable by using various process parameters configurations. The results proof the efficiency of the laser ablation as a pre-treatment even on the response to a cyclic loading. Based on this preliminary finding, the aim of the present work is to extend the characterization of the fatigue behavior of adhesively bonded joints by applying to a different geometry, namely the SLJ, the pre-treatments already experimented in [35]. The final goal of this work was to verify the level and the conditions of their capability to influence the lifetime of joints when tested with a cyclic loading. Two different substrates material were taken into account: (i) aluminium and (ii) stainless steel. The assessment of the fatigue life was conducted by evaluating the number of cycles to failure at different percentages of the static strength and by monitoring the crack initiation and propagation with visual microscopy.

2 Experimental setup

2.1 Materials and Joint geometry

The materials which were selected for the substrates were AA6082-T6 aluminium alloy and AISI 304 stainless steel, respectively, while a toughened two components epoxy adhesive, Loctite Hysol 9466, (Henkel, Düsseldorf - Germany) was employed for both the specimen families, regardless of the adherent material. The mechanical properties of the materials used for the manufacturing of the adherents are summarized in Table 1 and Table 2, respectively, while the adhesive properties are enumerated in Table 3

Table 1 – Aluminium AA6082-T6 mechanical properties (taken from the supplier certificate)

Property	Value
Young Modulus E_s	70 GPa
Poisson's ratio ν_s	0.33
Tensile yield strength Rp_s	295 MPa
Tensile ultimate strength Ru_s	320 MPa

Table 2 – AISI 304 stainless steel mechanical properties (taken from supplier certificate)

Property	Value
Young Modulus E_s	190 GPa
Poisson's ratio ν_s	0.29
Tensile yield strength Rp_s	230 MPa
Tensile ultimate strength Ru_s	510 MPa

Table 3 - Loctite Hysol 9466 mechanical properties (taken from www.henkel.com)

Property	Value
Young Modulus E_a	1718 MPa
Poisson's ratio ν_a	0.35
Tensile ultimate strength Ru_a (ASTM D 882)	32 MPa
Lap Shear Strength, ISO 4587:	
Aluminium substrates	26 MPa
Stainless steel substrates	23 MPa

The Single Lap Joint (SLJ) geometry was chosen to evaluate the changings in the fatigue response of the adhesively bonded joints according to the specific pre-treatment employed on the adherents before bonding them together. The dimensions of the joint, depicted in Figure 1, are provided in Table 4.

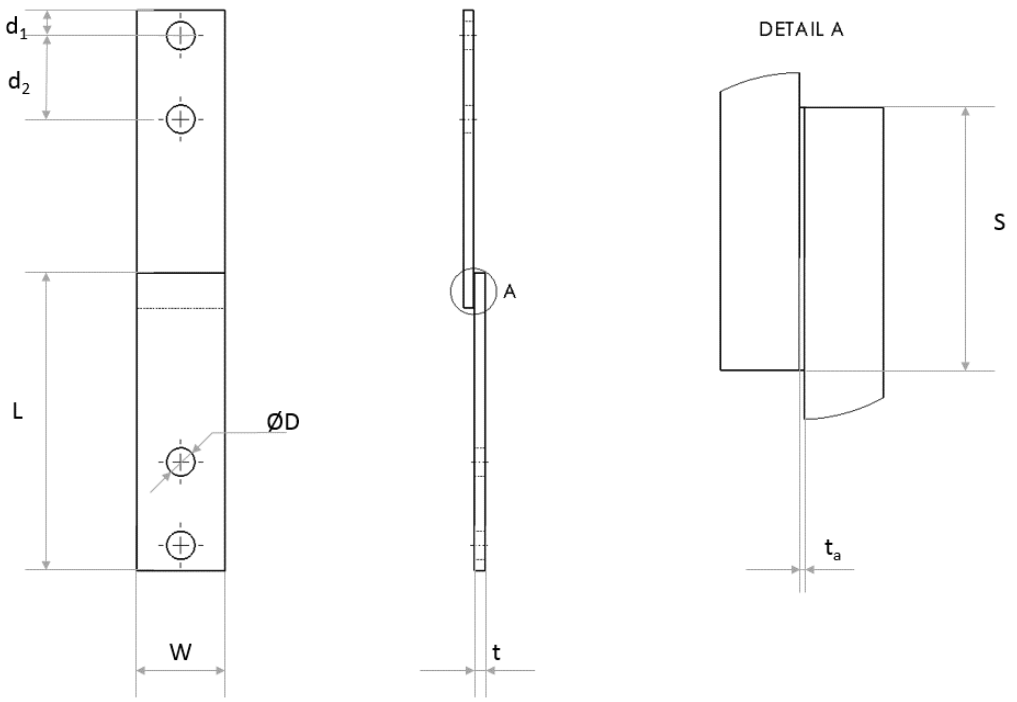

Figure 1 – SLJ geometry

Table 4 – SLJ dimensions

W (mm)	L (mm)	D (mm)	d_1 (mm)	d_2 (mm)	t (mm)	t_a (mm)	S (mm)
25	85	8	7.5	24	3	0.2	10

The value of the overlap length S was chosen after assuming higher values (S=15 mm and S=20 mm) which however resulted in the fatigue breakage of one of the substrates (especially for the aluminum alloy substrates) due to the tensile stress concentration in the proximity of the overlap.

2.2 Joint preparation

Firstly, the substrates were washed with soap and water in order to remove any trace of contaminants that can result from the machining. After this operation, several pre-treatments were carried out over the surfaces aimed to be bonded together. The aim was indeed to investigate the

possible differentiation in the fatigue behavior of the joints achievable through the application of different pre-treatments. The selected methods were the following:

(i). *Degreasing*: the substrate surfaces were cleaned with the Henkel 7063 chemical degreaser;

(ii). *Grit blasting*: the substrate surfaces underwent a grit blasting process with alumina particles (grade 80) at a pressure of 0.5 MPa and at a distance approximately equal to 30 mm from the nozzle and were finally treated with the same cleaner used to perform the simple degreasing;

(iii). *Laser ablation*: a Yb-fiber laser, featuring a z-axis positioning system for focus adjustment and a x-y galvo mirror scanner, was employed to ablate the surfaces of the substrates, using different combinations of process parameters.

Additional information is required to better illustrate the assumed criterion used to choose the different process configurations employed for the laser ablation. The combinations of laser ablation parameters were selected among the ones described in [35]. In particular, the index, whose variation was assumed to have a different effect over the mechanical behavior of the bonded joints previously pre-treated with laser ablation, was the energy density, ED, defined in the Eq. (1)

$$ED = \frac{P}{v\Phi_s} \tag{1}$$

where P is the laser nominal average power, v is the tangential scan speed and Φ_s is the nominal diameter of the spot (fixed to 35 μm). Other two significant parameters which can be varied to study their different influence on the quality of adhesion were the hatch distance, H, defined as the nominal distance between adjacent grooves from center to center of the laser beam induced spots, and the pulse repetition frequency, f, set to 20 kHz. From the experimental work carried out in [36] a peculiar trend of the critical value of the Mode I strain energy release rate of Double Cantilever Beam (DCB) joints by varying ED was found. According to that results, the fracture toughness of joints pre-treated with a low ED ablation process was very close to the one associated to simply degreased specimens. For higher values of ED, the capability of the laser ablation process to toughen the joints with respect to other traditional pre-treatments was strictly dependent from the value of hatch distance H employed. However, the overall trend remained untouched: the toughness

increased with ED until this one reached a threshold after which the toughness became decreasing when ED grew further up. The reason for this trend was ascribed to the fact that, when ED was lower than the threshold, the increase of the surface roughness with ED was determined by a prevalence of the height of the peaks with respect to the depth of the valleys, which resulted in an improvement of the interlocking effect between adhesive and substrate. Indeed, when ED overstepped the threshold, the depth of the valleys became more relevant than the height of the peaks, which led to a progressive entrapment of air inclusions within the grooves, worsening the adhesion phenomenon. When H was lower or approximately equal to the value of nominal spot diameter Φ_s, the toughness overstepped the value evaluated for the grit blasting specimens, until the energy density rose to the highest explored values. In the present work, the sensitivity to the hatch distance was explored only limited to two values (50 and 100 µm, respectively and one level of ED (ED=0.51 J/mm^2, obtained with P=18 W and v=1000 mm/s). With regard to the choice of the ED values used to perform the ablation, the levels were set in order to have some representative configurations of the whole range of values in which the mechanical behavior of the DCB joints was observed to significantly change. In particular, a low ED value (ED=0.17 J/mm^2), two medium values (ED=0.51 J/mm^2 and ED=1.14 J/mm^2, which were the values associated to the highest values of the fracture toughness of the DCB tests) and one high level (ED=5.71 J/mm^2) were set for the laser ablation. Table 5 summarizes the whole set of laser ablation process configurations employed for both the adopted materials.

Table 5 - Details of process parameters used for performing laser ablation over the substrates

Power [W]	Scan speed [mm/s]	ED [J/mm^2]	Hatch distance [µm]
6	1000	0.17	50
18	1000	0.51	50
18	1000	0.51	100
12	300	1.14	50
18	90	5.71	100

After being subjected to the pre-treatment, the substrates were bonded together with the previously described adhesive following the procedure defined in [37]. Some calibrated metal washers were used to keep the thickness of the adhesive in the overlap area fixed to 0.2 mm. The curing cycle was performed in a controlled climatic chamber, at 80°C for one hour, according to the instructions provided by the adhesive producer.

2.3 Surface morphology characterization

The evaluation of the surface morphology was based upon two main indexes, namely the surface roughness, S_a, and the Pearson's first coefficient of skewness, S_{sk}. According to ISO 25178-2:2012, the two indexes were evaluated with Eq. (2) and (3), respectively.

$$S_a = \frac{1}{A}\int\int |z(x,y)| dxdy \tag{2}$$

$$S_{sk} = \frac{1}{S_q^3 A}\int\int z^3(x,y) dxdy \tag{3}$$

In Eq. (3), S_q is the root mean square height of the surface, whose expression is provided in Eq. (4).

$$S_q = \sqrt{\frac{1}{A}\iint z^2(x,y) dxdy} \tag{4}$$

In particular, the coefficient of skewness S_{sk} represents the distribution of the peaks and valleys over the surface: positive values of the index mean that the height of the peaks was greater than the depth of the valleys with respect to the mean plane of the surface, while negative values of S_{sk} mean the opposite case.

In order to acquire the morphology maps of the surfaces, a CCI 3D optical profiler (Taylor-Hobson, Leicester, UK) with a resolution of 340 nm on the longitudinal plane and 1 nm on the vertical axis was used. For each pre-treatment, five 400μm x 400μm morphology maps were acquired and used for the parameters calculation.

2.4 Mechanical characterization

The fatigue tests were preceded by static tests aimed at determining the apparent shear strength of the joints, defined as in Eq. (5):

$$\tau_A = \frac{P_{MS}}{WS} \tag{5}$$

where P_{MS} is the maximum load reached during a quasi static tensile shear test over a SLJ specimen (an example of the Force vs. Displacement curve is shown in Figure 2), while W and S have been defined in Figure 1. The static tests were performed at room temperature, in a MTS 810 servo-

hydraulic machine (MTS Systems, Torino, Italy), equipped with a 100 kN load cell, in displacement control (1.3 mm/s), as prescribed by ASTM D1002. Three joints were tested for every combination of surface treatment and surface material; the only exception was represented by the stainless steel joint laser treated with ED = 0.51 J/mm^2 - H = 50 μm. Here eight specimens were tested due to an excessive scatter of the results of the first set of three specimens.

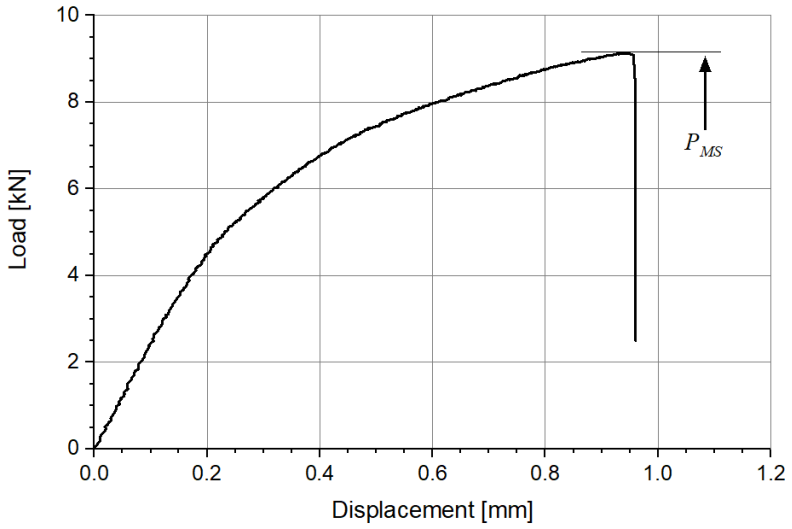

Figure 2 – Example a Load vs. Displacement curve, and definition of PMS

The subsequent fatigue tests were carried out using the same machine, in load control, by applying a load cycle with a repeated frequency f (constant and equal to 9 Hz) and a sinusoidal load wave with a load ratio R equal to 0.1. R is defined as the ratio between the minimum and the maximum values of the load cycle. The study was addressed to the finite life fatigue behaviour; therefore the load levels applied for each set of specimens (each set corresponded to a different substrate material and a different surface pre-treatment) were determined in order to obtain a number of cycles to failure in the range between 2'000 and 2'000'000.

The initiation and growth of the defects at the end of the overlap length were monitored by means of compliance evaluation and optical observation. The compliance of the specimens was continuously monitored during the fatigue test. Pictures of the side of the specimen were taken when the specimen compliance increased by 1% with respect to the initial value. Figure 3 shows an example of the optical observation of the side of the specimen during the fatigue test, at three different stages: beginning of the test (a), crack onset (b) and crack propagation (c).

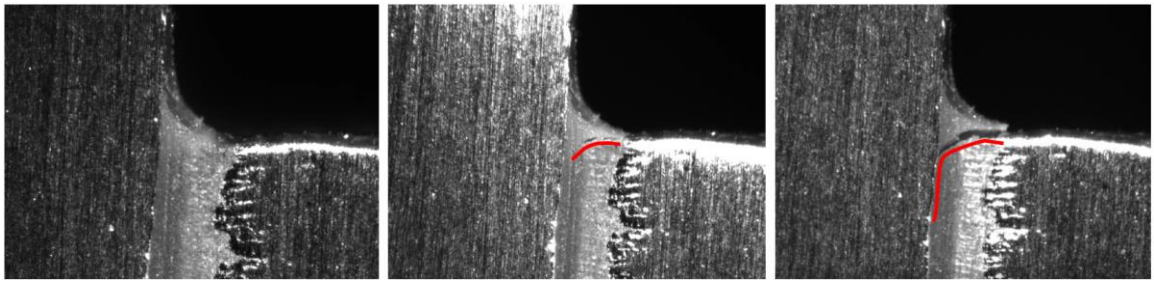

a) b) c)

Figure 3 – Example of optical observation of the crack growth: a) start of the test b) crack onset c) crack propagation

In particular, the crack initiation was identified when a small crack (size in the order of 0.1-0.2mm) could be clearly seen from the taken images. This identification allowed to distinguish the number of cycles to initiate a small defect (initiation) from the number of cycles required to completely break the joints.

3 Results and discussion

3.1 Surface morphology

Here the main results related to the changes induced on the surface morphology by the different performed pre-treatments are discussed. In particular, for what concerns the laser ablation, the surface showed a different topology according to the specific combination of lasing parameters employed, expressed by the energy density index and by the hatch distance value. The morphologies obtained on the AA6082-T6 substrates were already extensively discussed in a previous work of the authors [36]. For sake of comparison in Figure 4 and Figure 5 the morphology maps extracted on the degreased (a), the grit blasted (b) and two laser ablated (c, d) surfaces are provided for aluminum and stainless steel respectively.

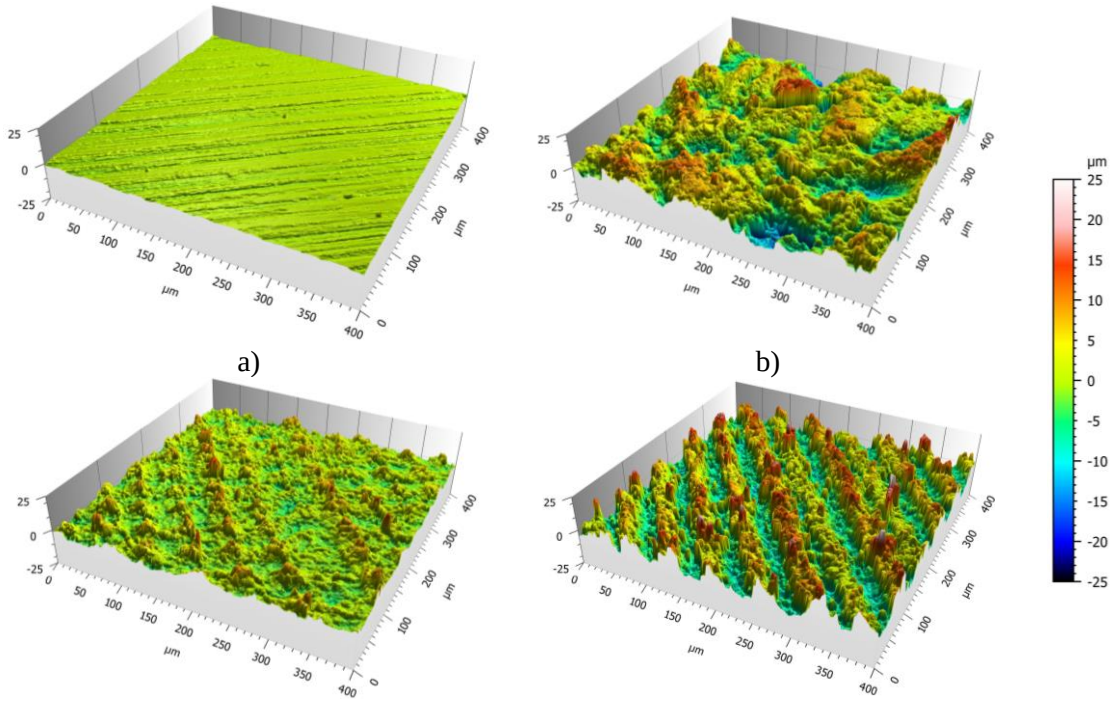

Figure 4 – Morphology maps of AA6082-T6 surfaces pre-treated with different processes: degreasing (a), grit blasting (b), laser ablation ED = 0.51 J/mm² (c), laser ablation ED = 1.14 J/mm² (d)

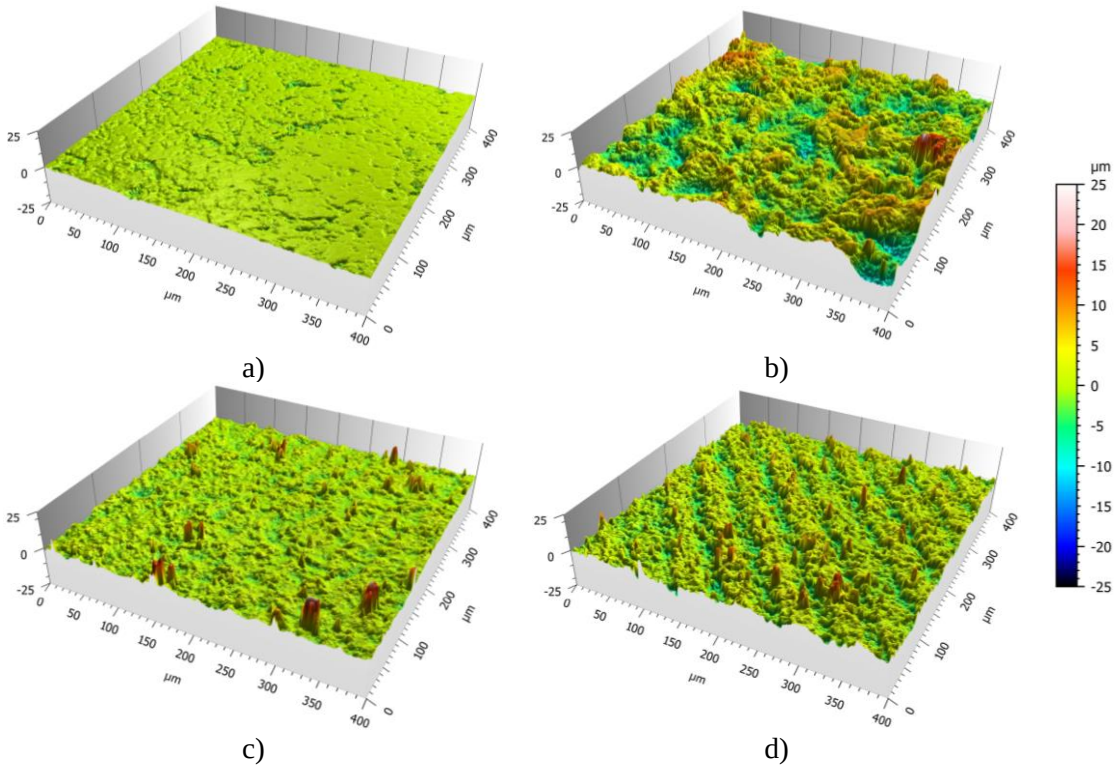

Figure 5 – Morphology maps of AISI 304 surfaces pre-treated with different processes: degreasing (a), grit blasting (b), laser ablation ED = 0.51 J/mm² (c), laser ablation ED = 1.14 J/mm² (d)

In Table 6, the parameters obtained for the considered surfaces are gathered. Moreover, Figure 6 shows the trend of average surface roughness (S_a) and skewness (S_{sk}) as a function of ED for the two considered materials for the laser treated surfaces.

Table 6 – Average values and standard deviation of Sa and Ssk parameters for the different surface treatments.

Material	Treatment	Sa [µm]		Ssk	
		AVG	*STD.DEV*	*AVG*	*STD.DEV*
AA 6082 T6	Degreasing	0.42	0.03	-0.08	0.72
	Grit Blasting	4.43	0.40	-0.62	0.09
	L.A. (ED=0.17 J/mm², H=50 µm)	0.98	0.13	-0.32	0.36
	L.A. (ED=0.51 J/mm², H=50 µm)	4.24	0.13	0.72	0.03
	L.A. (ED=0.51 J/mm², H=100 µm)	2.60	0.06	-0.14	0.14
	L.A. (ED=1.14 J/mm², H=50 µm)	5.18	0.11	0.16	0.04
	L.A. (ED=5.71 J/mm², H=50 µm)	11.78	0.19	-0.64	0.07
AISI 304	Degreasing	0.39	0.02	-2.73	0.32
	Grit Blasting	2.98	0.27	-0.20	0.20
	L.A. (ED=0.17 J/mm², H=50 µm)	1.14	0.04	0.75	0.26
	L.A. (ED=0.51 J/mm², H=50 µm)	0.94	0.04	2.71	0.97
	L.A. (ED=0.51 J/mm², H=100 µm)	1.31	0.02	0.48	0.09
	L.A. (ED=1.14 J/mm², H=50 µm)	1.81	0.06	0.62	0.23
	L.A. (ED=5.71 J/mm², H=50 µm)	7.54	0.72	0.10	0.04

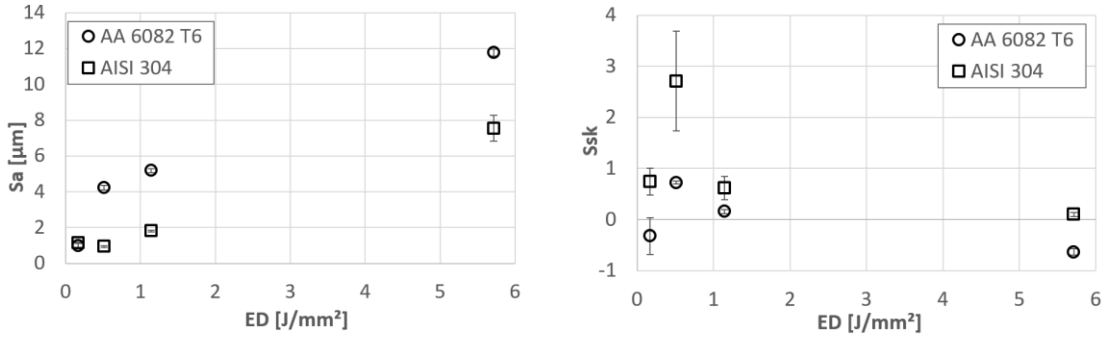

a) b)

Figure 6 – Surface average roughness (Sa) and Skewness coefficient (Ssk) trend as a function of the energy density for the laser treated aluminum and stainless steel surfaces

The degreased surfaces showed a smooth profile while the grit blasted ones presented a rougher appearance, which was confirmed by the values of surface roughness S_a. This outcome is consistent with the values documented for cold rolled sheets [38] and grit blasted surfaces [39], respectively. The corresponding value of surface skewness, S_{sk}, for the aluminum degreased surface was close to zero, pointing out the symmetry of the distribution of the small asperities over the surfaces. The same index for the stainless steel substrates was lower then zero due to the surface morphology produced by the rolling process, characterized by a sort of flat surface with some small hollows (Figure 5a).

For both, the aluminum and stainless steel grit blasted surfaces, the Ssk coefficients were slightly lower than zero, resulting in a sort of random surface marked by a weak presence of valleys. By analysing the effect of the laser ablation over the surface morphology, for the two materials, it is possible to notice how the changes were very sensitive to the value of energy density ED employed to perform the treatment. As an outcome, the surface roughness S_a was found to grow up with the energy density ED for the range of parameters considered in this work. Moreover, it can be noticed that for the same ED value, the aluminum surfaces appeared rougher. This result pointeds out that for the same level of density of energy given to the surface, a greater volume of material was ablated if compared with stainless steel. The trend of the surface skewness represents how the lasing energy employed for unit area was capable to induce a surface morphology characterized by the presence of peaks or, on the contrary, by the prevalence of valleys. As already discussed in [36] for aluminum substrates, also stainless steel surfaces shown an increase of Ssk rising up ED from 0.17 J/mm^2 to 0.51 J/mm^2. When ED was risen to 0.51 J/mm^2 the ablation succeeded in significantly modifying the surface topology, resulting in a prevalence of peaks due to the stacking of melted material generated by the superimposition between adjacent grooves. As ED further grew up, the higher amount of energy provided to the surface was able to induce increasingly deeper grooves, producing a surface morphology characterized by the prevalence of valleys rather than peaks. Although the specific values of Sa and Ssk for the two materials were quite different, the global trend was maintained.

3.2 Static tests

The results related to the static tests are summarized in Table 7 and Table 8, for AA6082-T6 and AISI604 respectively. The specimens are distinguished according to the pre-treatments which they underwent and, with specific regard to the laser ablation pre-processing, to the combination of parameters used to perform the treatment. The values of apparent shear strength were averaged on at least three specimens for each set.

Table 7 - AA6082 T6 SLJ static test results ("L.A" stands for "Laser Ablation")

Pre-treatment	**τ_A (MPa)**	**St. dev. (MPa)**	**Failure mode**
Degreasing	30.04	1.93	Adhesive
Grit blasting	36.39	0.25	Mostly Adhesive
L.A. (ED=0.17 J/mm^2, H=50 µm)	39.18	0.70	Mixed Adhesive/Cohesive
L.A. (ED=0.51 J/mm^2, H=50 µm)	42.52	0.66	Mixed Adhesive/Cohesive
L.A. (ED=0.51 J/mm^2, H=100 µm)	43.29	0.27	Mixed Adhesive/Cohesive
L.A. (ED=1.14 J/mm^2, H=50 µm)	38.83	1.21	Mostly Cohesive
L.A. (ED=5.71 J/mm^2, H=50 µm)	34.26	1.85	Cohesive

Table 8 - AISI 604 SLJ static test results ("L.A" stands for "Laser Ablation")

Pre-treatment	**τ_A (MPa)**	**St. dev. (MPa)**	**Failure mode**
Degreasing	29.19	0.97	Adhesive
Grit blasting	34.94	2.48	Adhesive
L.A. (ED=0.17 J/mm^2, H=50 µm)	36.04	0.82	Mostly Adhesive
L.A. (ED=0.51 J/mm^2, H=50 µm)	42.03	2.68	Mixed Adhesive/Cohesive
L.A. (ED=0.51 J/mm^2, H=100 µm)	41.81	0.51	Mixed Adhesive/Cohesive
L.A. (ED=1.14 J/mm^2, H=50 µm)	46.02	0.68	Cohesive
L.A. (ED=5.71 J/mm^2, H=50 µm)	40.15	0.48	Cohesive

The graphs in Figure 7Figure 7 *a* and *b* depict the trend of the apparent shear strength τ_A with ED for the aluminium and the stainless steel cases, respectively, comparing the values of the laser ablated specimens with the results of the degreased and the grit blasted samples.

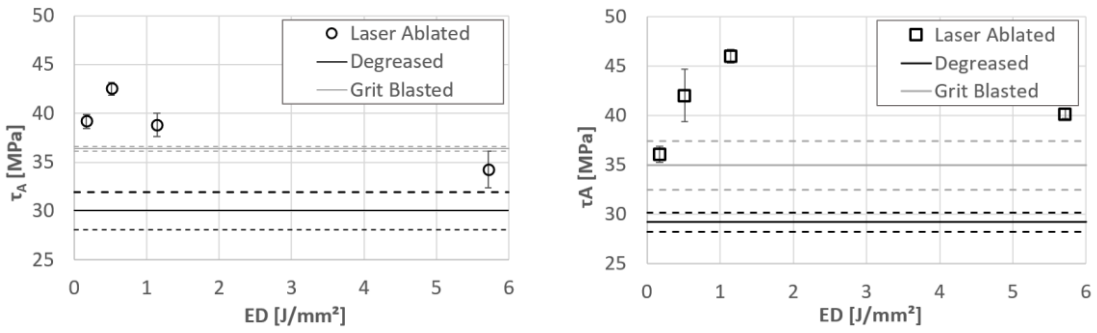

Figure 7 – Trend of quasi static apparent shear strength vs energy density employed for the laser ablation for aluminum (a) and stainless steel joints (b). The degreased and the grit blasted values are reported for comparison purposes.

For both the cases, the apparent shear strength trend resulted consistent with the one of the fracture toughness G_{IC} identified in [36] with a significant difference: even a low ED treatment in this case was able to increase the value of τ_A with respect to the correspondent value exhibited by the simply degreased specimens. The apparent shear strength then, as ED further grew up, increased and then fell after the overcoming of a threshold value of ED.

Again in Figure 8 and Figure 9 the apparent average shear strength is plotted against the average surface roughness and the surface skewness, respectively, for the two material considered.

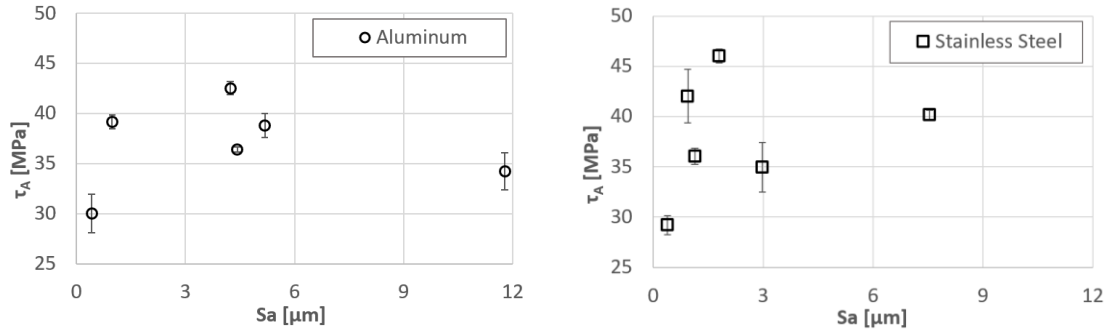

Figure 8 – Trend of quasi static apparent shear strength vs the average surface roughness Sa, for the entire set of surface treatment considered and aluminum (a) and stainless steel (b) substrates.

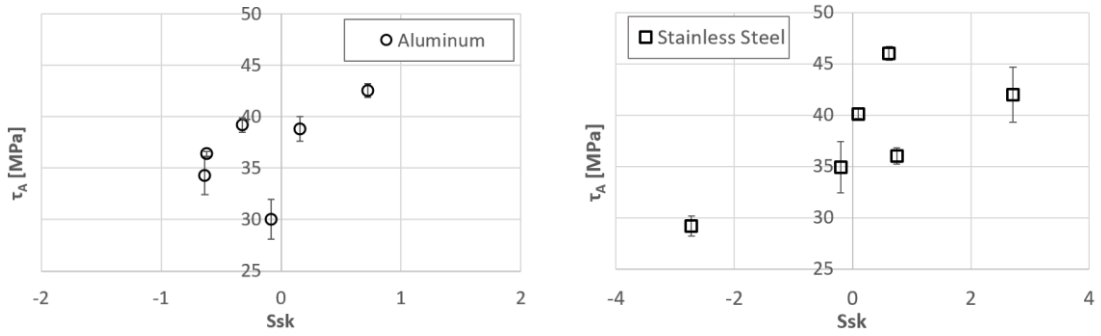

Figure 9 – Trend of quasi static apparent shear strength vs the surface skewness Ssk, for the entire set of surface treatment considered and aluminum (a) and stainless steel (b) substrates.

As already found in [36] it appears that the average surface roughness (Sa) did not represent a good indicator of the joint strength, while, on the opposite, it appeared that the average shear strength tended to grow up when the surface skewness increased. It should also be noticed as the shear strength of stainless steel joints treated with ED = 0.51 J/mm^2 - H = 50 μm resulted affected by a standard deviation significantly higher then the other laser treated joints. This particular aspect was detectable even in the skewness coefficient associated to the same combination of parameters (see Figure 6). Based on these results a possible correlation between Ssk and $\tau_{A,}$ can be detected. Thus, the fact that both the results presented an high data dispersion allows to state that, when a specific laser configuration was applied, the mechanical performance was extremely sensitive to the surface morphology in terms of distribution of peaks and valleys, which further validated the detected correlation between the two quantities. Therefore, even considering the closeness of the mean surface roughness to the values associated to lower ED treated specimens, the treatment was confirmed to represent a threshold both for the mechanical resistance and for the type of modification produced over the surface morphology by the laser ablation.

With regard to the aluminium substrates case, Figure 10 provides representative examples of how the fracture surface appeared in every class of specimens. The appearance of the fracture surface was diversified according to the pre-treatment and, for the laser ablation case, to the employed process configuration. In particular, while the surface of the adhesive detached from one substrate in the degreased and, for the most of the surface, in the grit blasted specimens, a more cohesive failure took place for the laser treated specimens. In the laser ablated samples with ED=0.51 J/mm^2, H=50 μm and H=100 μm, the failure surfaces were smooth and the crack mostly propagated in the proximity of the metal-adhesive interface, leaving only a thin adhesive layer on one of the two

metal substrates. For the joints treated with ED=0.17 J/mm^2 and ED=1.14 J/mm^2 the fracture surfaces appeared characterized by a significantly jagged surface, with the crack propagating from the proximity of one interface to the other for the whole overlap length and the adhesive being snatched from one surface to the other. The set with ED=5.71 J/mm^2 showed a completely cohesive failure with a sort of "archipelago" fracture surface, characterized by a distribution of many small portions of adhesive remaining attached on the substrate surface. Although here the fracture was fully cohesive, as demonstrated in [40], the fracture surfaces was characterized by a significant porosity due to the air entrapped in the deep ablation induced valleys.

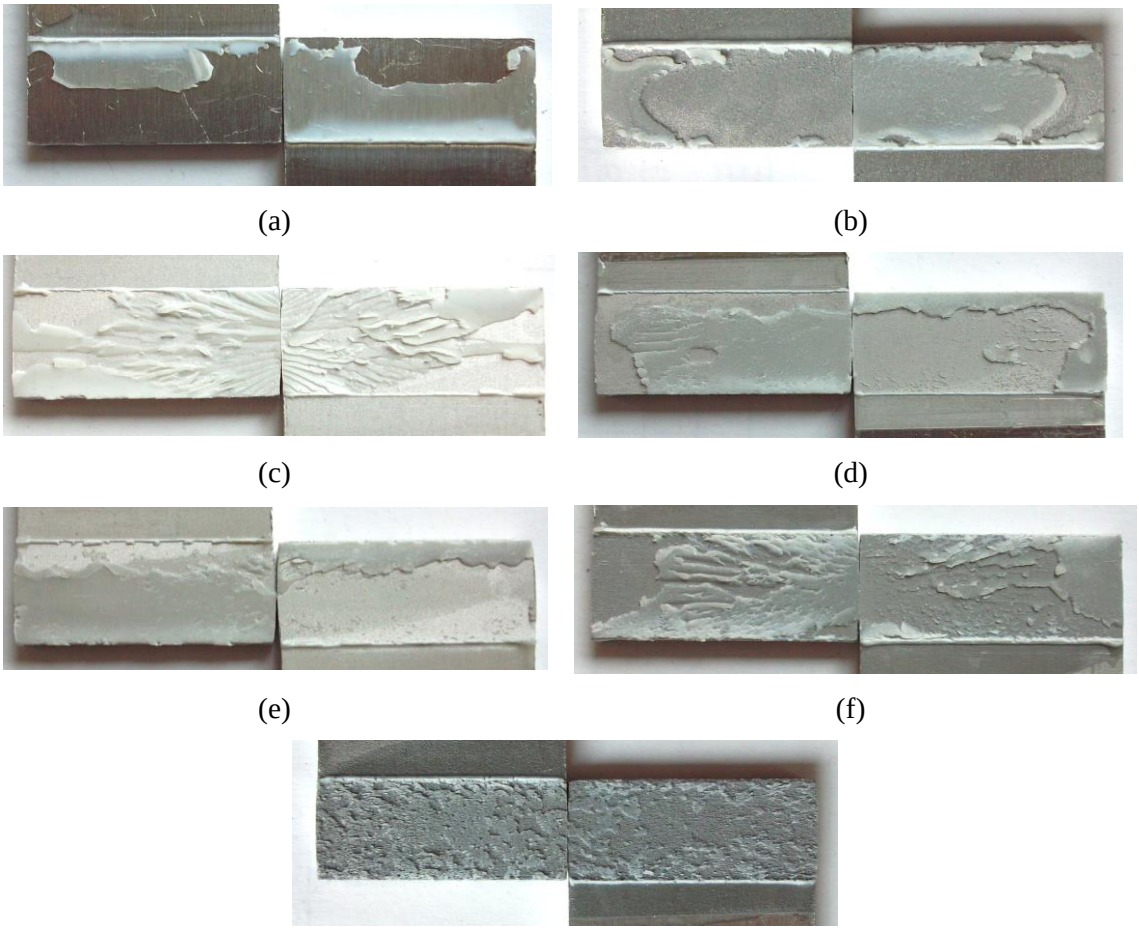

Figure 10 - Fracture surfaces of AA6082-T6 SLJ subjected to quasi-static tensile test: (a) degreased; (b) grit blasted); (c) ED=0.17 J/mm^2(H=50 µm); (d) ED=0.51 J/mm^2 (H=50 µm); (e) ED=0.51 J/mm^2 (H=100 µm); (f) ED=1.14 J/mm^2 (H=50 µm); (g) ED=5.71 J/mm^2 (H=50 µm)

In the case of the stainless steel substrates (Figure 11), the degreased and grit blasted joints presented a complete interfacial failure, characterized by at most one switch of side on which the crack propagated. All the laser ablated specimens showed an indented surface of the detached adhesive and a more winding crack path along both the interfaces. Predominately adhesive failures were found for the specimens ablated with an ED equal to 0.171 J/mm². The fracture became progressively more cohesive for the laser ablated specimens with higher ED values. In particular, for ED 1.14 J/mm² and 5.71 J/mm² fully cohesive failures were found, although the fracture propagated in the proximity of the metal – adhesive interface.

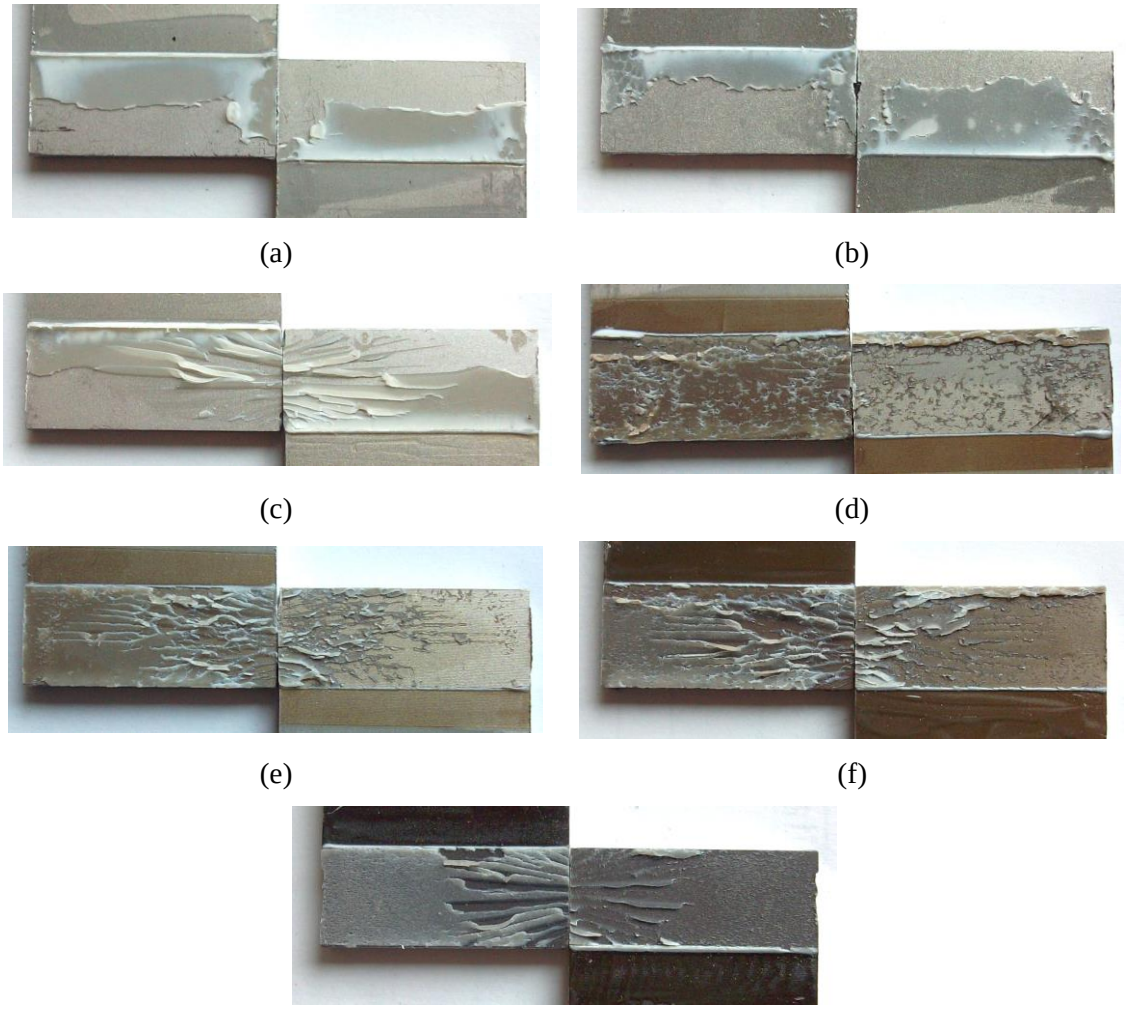

Figure 11 - Fracture surfaces of AISI 304 SLJ subjected to quasi-static tensile test: (a) degreased; (b) grit blasted); (c) ED=0.17 J/mm²(H=50 µm); (d) ED=0.51 J/mm² (H=50 µm); (e) ED=0.51 J/mm² (H=100 µm); (f) ED=1.14 J/mm² (H=50 µm); (g) ED=5.71 J/mm² (H=50 µm)

3.3 Cyclic loading tests

The effect of the experimented pre-treatments and, with specific refer to the laser ablation, of the employed combination of process parameters was investigated by means of the stress-life approach. For each specimen, the fatigue curve was drawn considering the maximum component of apparent shear stress acting during the loading cycle over the adhesively bonded area, τ_{max}, and the number of cycles to failure, N_f, corresponding to the complete separation of the substrates. The fatigue data were plotted considering a log-normal distribution of the number of cycles to failure according to Eq. (8).

$$N_f \tau_{max}^{\mu} = k \tag{8}$$

The double logarithmic graph in Figure 12 offers a first snapshot of the results for the aluminium substrates case. For each set, the confidence bands for both 10% and 90% failure probability and for a 90% confidence level, according to ISO 12107, were provided.

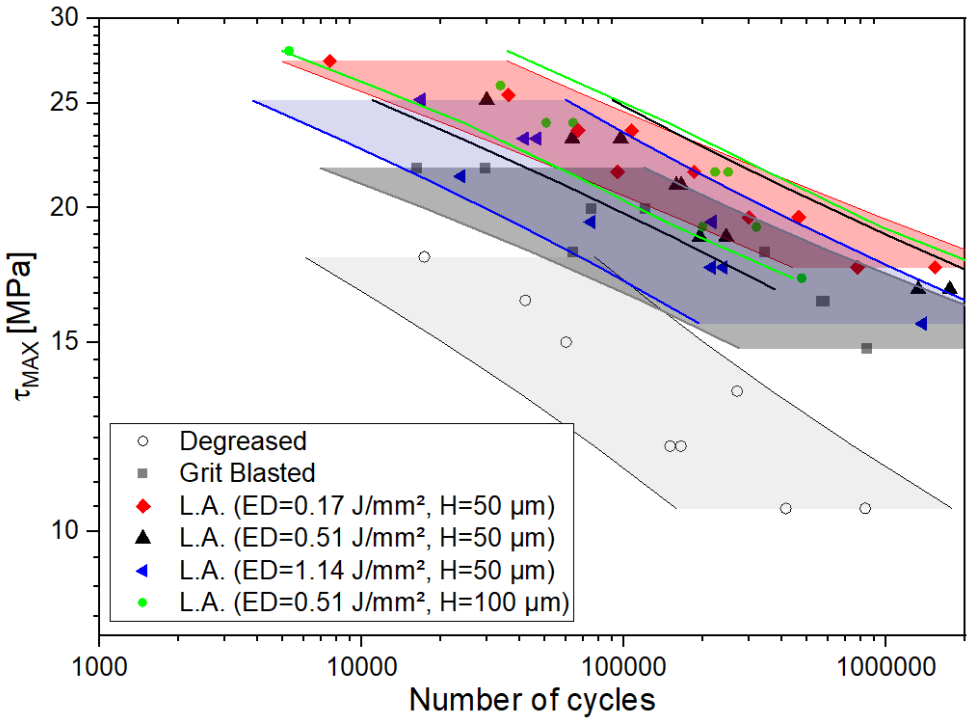

Figure 12 – S-N curves for fatigue tested SLJ with aluminium substrates (the continuous lines are the power law trend lines for every group of specimens). The sets without information about the values of the hatch distance in the legend presented H=50µm. The confidence bands (10% and 90% failure probability, 90% confidence level) are provided for each set (some ranges between the confidence bands are coloured to improve the readability)

In Table 9 the values of the inverse slope μ and of the intercept $k^{1/\mu}$ of the fatigue curve, for every set of aluminium specimens, as well as their coefficient of determination R^2, are listed.

Table 9 – Inverse slope, intercept and coefficient of determination for every group of specimens with AA6082-T6 substrates, differentiated according to the pre-treatment which they underwent

Pre-treatment	**μ [1/ln(MPa)]**	**$k^{1/\mu}$ [MPa]**	**R^2 [-]**
Degreasing	6.76	76.26	0.88
Grit blasting	11.36	52.29	0.85
L.A. (ED=0.17 J/mm^2, H=50 μm)	10.24	68.38	0.91
L.A. (ED=0.51 J/mm^2, H=50 μm)	9.52	73.49	0.91
L.A. (ED=0.51 J/mm^2, H=100 μm)	9.80	71.43	0.85
L.A. (ED=1.14 J/mm^2, H=50 μm)	9.52	67.35	0.86
L.A. (ED=5.71 J/mm^2, H=50 μm)	-	-	-

Firstly, it is worth noting that the curve associated to the degreased samples was the lowest of the whole experimented sets, indicating the lowest fatigue strength. Similarly to the quasi static test, the fracture surfaces resulted in a fully adhesive failure (Figure 13). With reference to the grit blasted joints, their fatigue strength was significantly higher than those of degreased joints and slightly lower than the laser ablated ones, accordingly to the quasi static tests. Their fracture surfaces were characterized again by a predominantly adhesive failure. The laser ablated samples presented in general the best results in terms of number of cycles to failure.

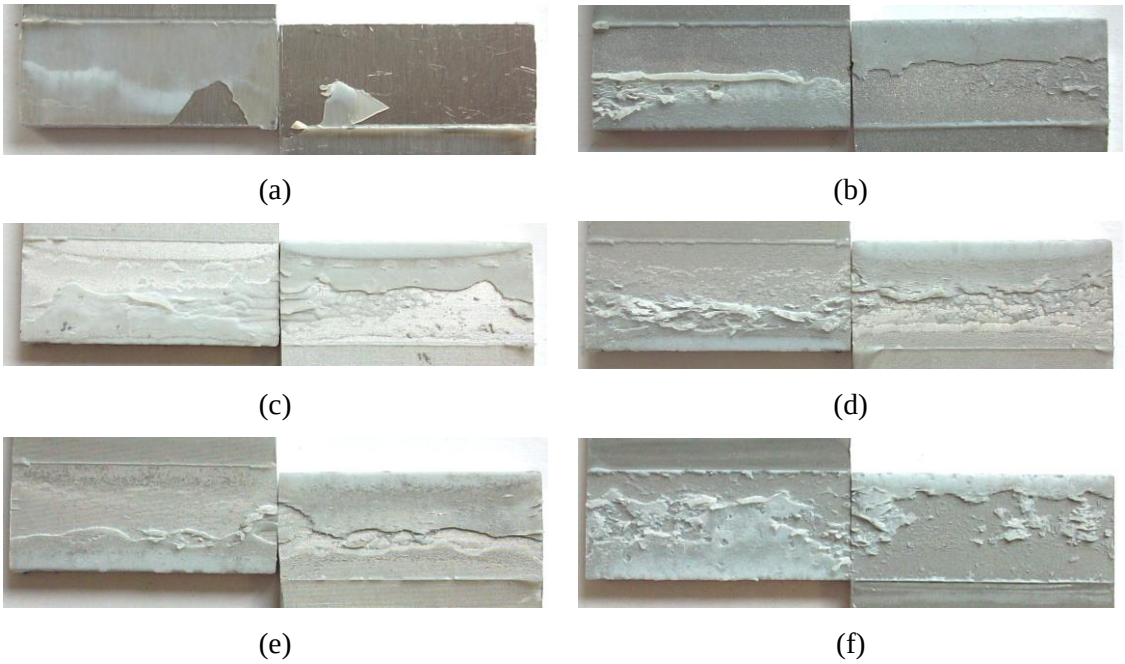

Figure 13 - Fracture surfaces of AA6082-T6 SLJ subjected to fatigue test: (a) degreased; (b) grit blasted); (c) ED=0.17 J/mm^2(H=50 µm); (d) ED=0.51 J/mm^2 (H=50 µm); (e) ED=0.51 J/mm^2 (H=100 µm); (f) ED=1.14 J/mm^2 (H=50 µm).

All the laser treated joints, regardless to the level of energy density used to perform the ablation, presented approximately the same results in terms of fatigue resistance, with two exceptions:

i. the set pre-treated with ED=5.71 J/mm^2 always presented breakage in correspondence of the aluminium substrates (this is the reason because this set does not present any data in Table 9). The laser treatment performed at this energy density level produced very deep groves that acted as defect for the aluminum plates, yielding the breakage of the aluminum rather than those of the adhesive layer.
ii. the set pre-treated with ED=1.41 J/mm^2 presented a fatigue strength slightly lower than the other laser treated specimens. This aspect was related to the presence of a certain porosity, consequence of the entrapment of bubbles in the deepest valleys of the surface during the adhesive deposition [36].

The failure surface of specimens pre-treated with ED = 0.17 J/mm² and 0.51 J/mm² (for both H = 50 and H = 100µm) is presented in Figure 14. They were characterized by an initial propagation of the crack within the adhesive, in the proximity of the metal-polymer interface, and followed by the final, quasi static failure presenting a mixed adhesive/cohesive failure surface.

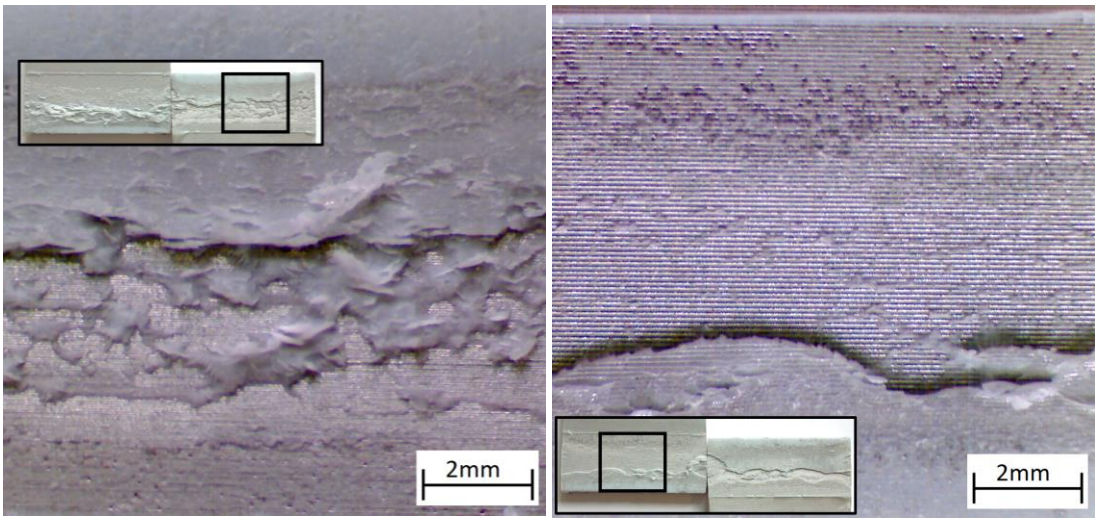

a) b)

Figure 14 – Detail of the fracture surfaces of AA6082-T6 SLJ subjected to fatigue test: a) ED=0.51 J/mm^2, H=50 µm, b) ED=0.51 J/mm^2, H=100 µm

The S-N diagram with the results of the fatigue tests on the stainless steel joints is depicted in Figure 15 and the regression coefficients are listed in Table 10. Representative surfaces fracture of stainless still fatigue tested joints are gathered in Figure 16.

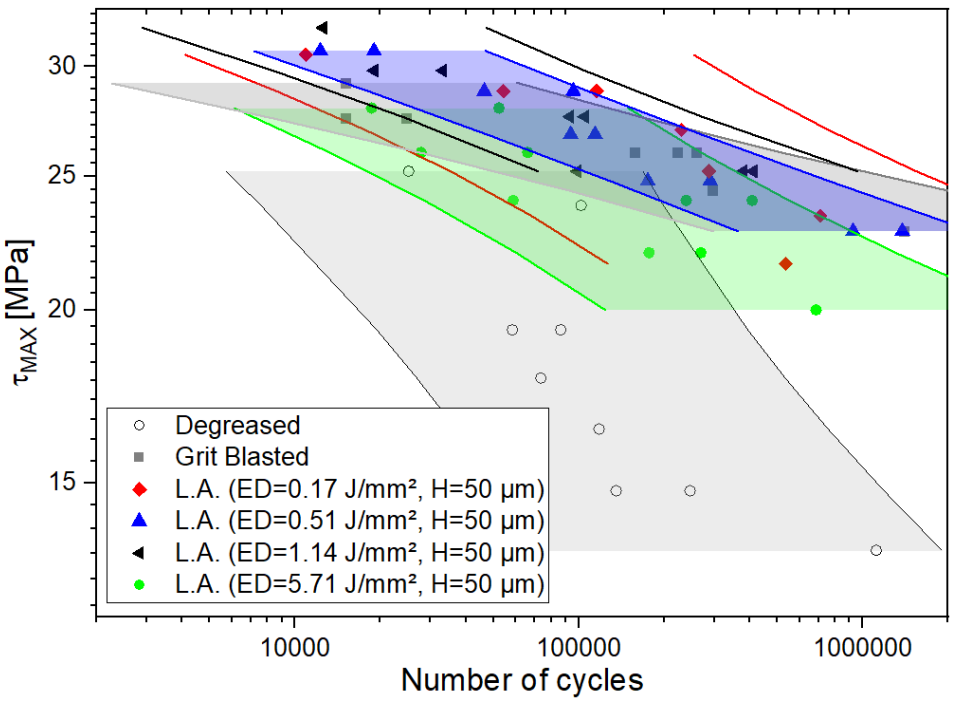

Figure 15- S-N curves for fatigue tested SLJ with stainless steel substrates (the continuous lines are the power law trend lines for every group of specimens). The confidence bands (10% and 90% failure probability, 90% confidence level) are provided for each set (some ranges between the confidence bands are coloured to improve the readability)

Table 10 - Inverse slope, intercept and coefficient of determination for every group of specimens with AISI 304 substrates, differentiated according to the pre-treatment which they underwent

Pre-treatment	**µ** **[1/ln(MPa)]**	**$k^{1/\mu}$** **[MPa]**	**R^2** **[-]**
Degreasing	6.02	124.1	0.65
Grit blasting	22.72	43.38	0.88
L.A. (ED=0.17 J/mm^2, H=50 µm)	13.16	65.30	0.78
L.A. (ED=0.51 J/mm^2, H=50 µm)	15.15	58.26	0.86
L.A. (ED=1.14 J/mm^2, H=50 µm)	13.89	61.65	0.94
L.A. (ED=5.71 J/mm^2, H=50 µm)	12.99	59.36	0.71

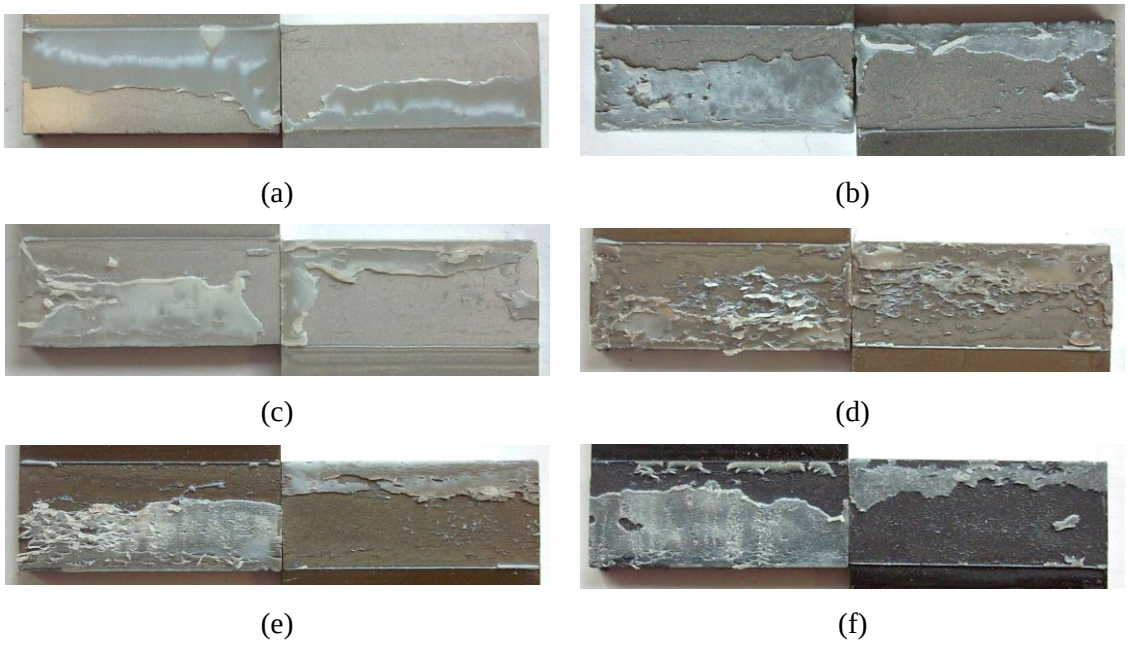

Figure 16 - Fracture surfaces of AISI 304 SLJ subjected to fatigue test: (a) degreased; (b) grit blasted); (c) ED=0.17 J/mm2(H=50 µm); (d) ED=0.51 J/mm2 (H=50 µm); (e) ED=1.14 J/mm2 (H=50 µm); (f) ED=5.71 J/mm2 (H=50 µm)

As already shown for the aluminum joints, the degreased SLJ showed a completely adhesive failure and, as a consequence, yielded the worst fatigue strength. As shown in Figure 17, the grit blasted joints showed a predominately adhesive fracture surface with some small cohesive portions. They performed therefore significantly better than the degreased samples and their fatigue strength was comparable with those of the laser ablated joints.

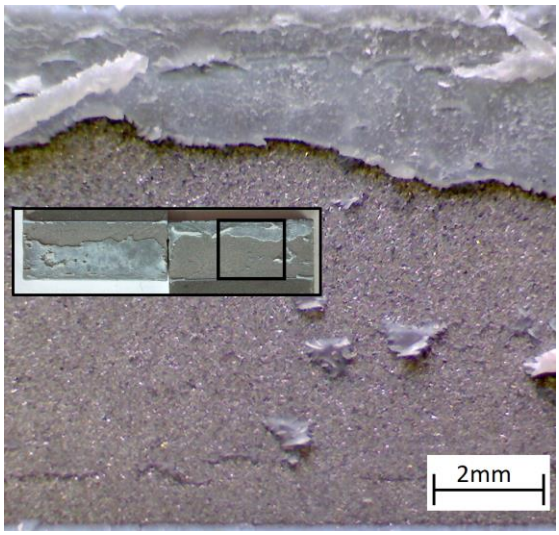

Figure 17 – Detail of the fracture surfaces of AISI 304 Grit Blasted SLJ subjected to fatigue test.

The laser ablated SLJ with ED = 0.17 / 0.51 and 1.14 J/mm² gave the best fatigue performance and no significant difference can be found in the S-N plot among these three data sets.

Examples of their fracture surfaces are shown in Figure 18. It can be noticed that the fractures propagated in the adhesive layer near the polymer-metal interface. Moreover, also some areas with cohesive failure can be found: this is an indicator of the strong interaction between the substrates and the adhesive produced by the laser treatment.

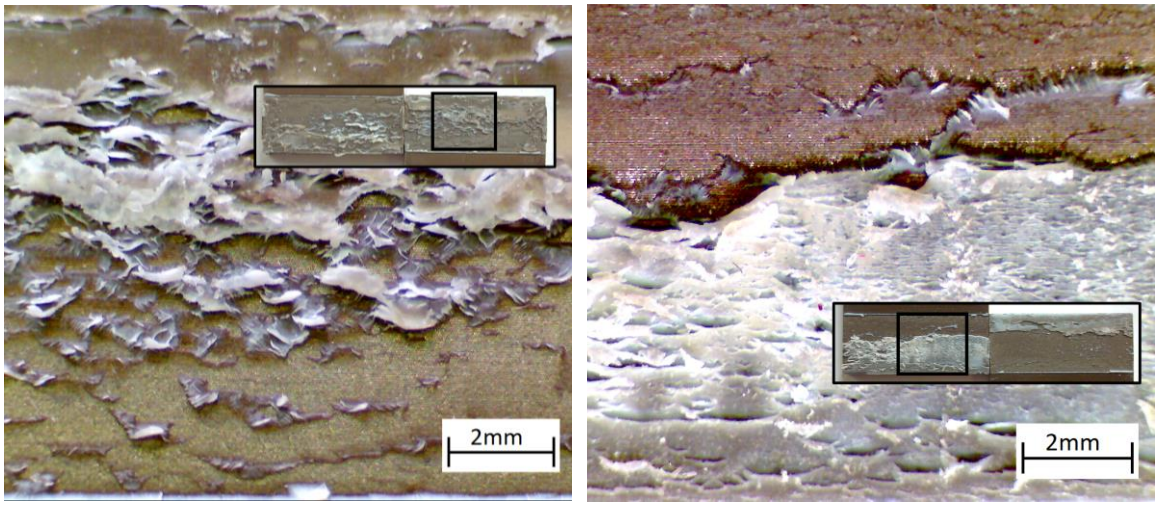

a) b)

Figure 18 – Detail of the fracture surfaces of AISI 304 SLJ subjected to fatigue test: a) ED=0.51 J/mm², H=50 µm, b) ED = 1.14 J/mm², H=50 µm

The laser ablated joints with ED = 5.71 J/mm² yielded a lower fatigue strength if compared with the other laser ablated joints, although they showed a macroscopically cohesive failure. By analyzing more in detail their fracture surface (Figure 19), it can be noticed that a certain porosity can be found (indicated by the black arrows). This was a consequence of the air entrapped in the deepest grooves produced by the laser treatment performed with high ED levels.

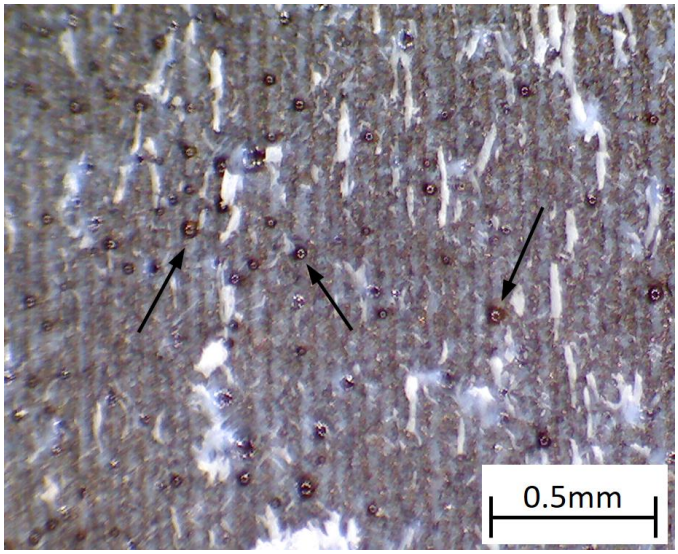

Figure 19 – Detail of the fracture surfaces of AISI 304 SLJ subjected to fatigue test (ED=5.71 J/mm², H=50 µm). Black arrows indicate the presence of air bubbles

The identification of the crack initiation allowed to separate the entire life of each specimen in number of cycles spent to initiate the defect and number of cycles spent to propagate the defect. By comparing initiation and failure number of cycles of two different data sets, the influence of the surface pre-treatment on the defect initiation and defect propagation can be understood. This analysis is shown in Figure 20 for grit blasted and laser ablated (ED = 0.17 J/mm², H = 50 μm) aluminum joints. As shown above, the laser ablated joints (black filled circles) always yielded a higher number of cycles at failure than the grit blasted ones (black filled squares) for a certain level of applied shear stress. This ranking cannot be found for the initiation since the points related to the initiation of laser ablated joints (black hollow circles) seemed to be blended into those related to the initiation of grit blasted ones (black hollow squares). For example, if an applied shear stress of approximately 21.5 MPa is considered, the initiation of both laser ablated and grit blasted joints, took place, within a range of 2'500 – 9'000 cycles, while the final failure took place approximately at 90/200'000 and 16/30'000 cycles for laser ablated and grit blasted joints respectively. This behavior clearly indicates that the surface pre-treatment did not significantly affect the initiation time, while it had a strong influence of the total fatigue life, and therefore on the propagation stage.

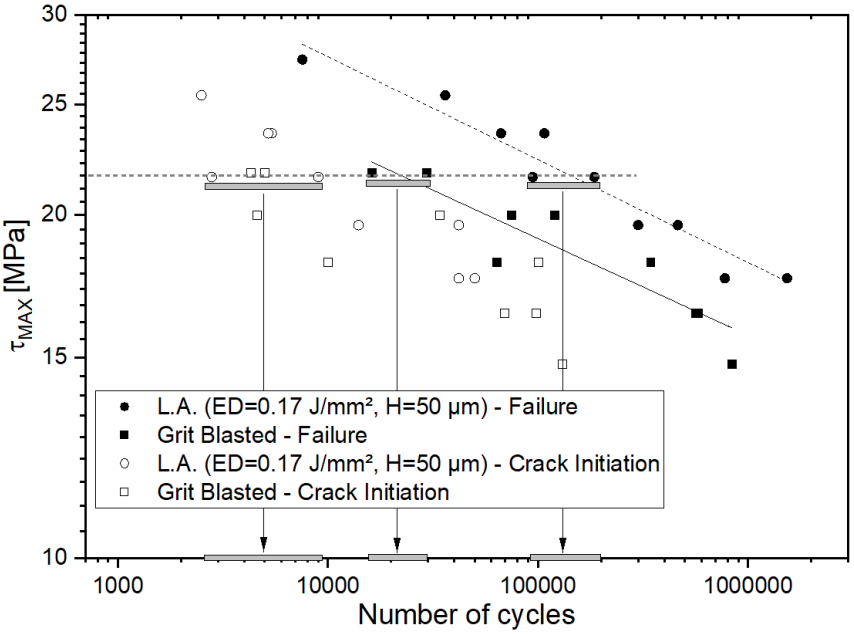

Figure 20- Comparison between crack initiation and failure of Grit Blasted and Laser Ablated (ED=0.17 J/mm², H=50µm) fatigue tested aluminum SLJ.

The same comparison is carried out for stainless steel joint pre-treated with two different levels of ED (0.51 J/mm² and 5.71 J/mm²). Here, again, the initiation seems to be independent from the surface treatment, while the defect propagation (until the final failure) of laser ablated joints with ED = 0.51 J/mm² required a greater number of cycles if compared with that of laser ablated joints with ED = 5.71 J/mm².

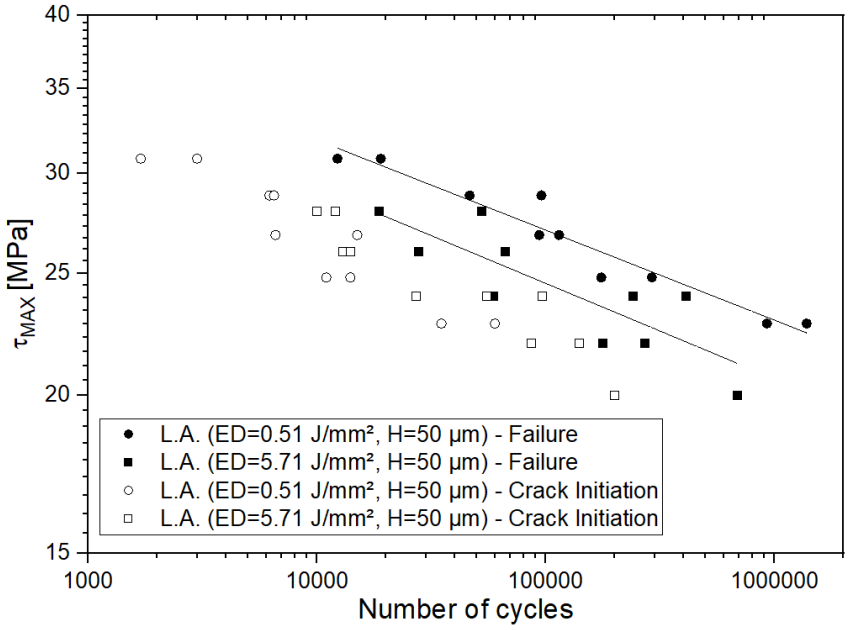

Figure 21- Comparison between crack initiation and failure of Laser Ablated ED=0.51 J/mm², H=50µm and ED=5.71 J/mm², H=50µm, fatigue tested aluminum SLJ.

4 Conclusions

In this work, the influence of the surface morphology produced by different surface pre-treatment on the quasi static and fatigue strength of aluminum and stainless steel single lap joints was investigated. The result of the quasi static test indicated that the higher apparent average shear strength was yielded by the laser ablated specimens, in particular with and ED equal to 0.51 J/mm² and 1.14 J/mm² for aluminum and stainless steel substrates respectively. The laser pretreatment allowed an increase in the joint strength approximately of 50% if compared with degreased joints and of the 25% if compared with the grit blasted ones. Concerning the fatigue behavior, the laser treated joints performed significantly better than the degreased and the grit blasted ones in the case of aluminum substrates. The exceptions were represented by the laser treatments performed with the higher energy density level, where a certain porosity was found in the adhesive layer, affecting the joint strength. By the compliance and optical monitoring, the crack initiations were detected. For each specimen, it was therefore possible to distinguish the time spent for the initiation and the time spent for the propagation of the crack. The result pointed out that the crack initiation was almost independent by the surface treatment, while the higher fatigue life shown by the laser treated joint was strongly related to their longer propagation stage.

Acknowledgments

This research was supported by the Italian Ministry for University and Research (MIUR), grant SIR RBSI146ZYJ.

References

1. Kinloch AJ. Adhesion and adhesives: Science and technology. New York: Chapman and Hall; 1987
2. Costa M, Viana G, da Silva LFM, Campilho RDSG. Environmental effect on the fatigue degradation of adhesive joints: a review. J Adhes 2017;93(1-2):127-46
3. Mostovoy S, Ripling E, Lee LH. Adhesion Science and Technology, vol. 9B. New York: Plenum Press; 1975
4. Reedy Jr EF. Free-edge stress intensity factor for a bonded ductile layer subjected to shear. J Appl Mech 1993;60:715-20
5. Wang CH, Rose LRF. Compact solutions for the corner singularity in bonded lap joints. Int J Adhes Adhes 2000;20:145-54
6. Imanaka M, Ishii K, Nakayama H. Evaluation of fatigue strength of adhesively bonded single and single step double lap joints based on stress singularity parameters. Eng Fract Mech 1999;62 (4-5):409-24
7. Shenoy V, Aschcroft IA, Critchlow GW, Crocombe AD, Abdel Wahab MM. An investigation into the crack initiation and propagation behavior of bonded single-lap joints using backface strain. Int J Adhes Adhes2009;29 (4):361-71
8. Zhang Z, Shang JK, Lawrence FV. A backface strain technique for detecting fatigue crack initiation in adhesive joints. J Adhes 1995;49 (1-2):23-36
9. Graner Solana A, Crocombe AD, Aschcroft IA. Fatigue life and backface strain predictions in adhesively bonded joints. Int J Adhes Adhes 2010;30 (1):36-42
10. Deng J, Lee MMK. Fatigue performance of metallic beam strengthened with a bonded CFRP plate. Comp Struct 2007;78 (2):222-31
11. Harris JA, Fay PA. Fatigue life evaluation of structural adhesives for automotive applications. Int J Adhes Adhes 1992;12 (1):9-18
12. Quaresimin M, Ricotta M. Fatigue behaviour and damage evolution of single lap bonded joints in composite material. Compos Sci Technol 2006;66:176-87
13. Curley AJ., Hadavinia H, Kinloch AJ, Taylor AC. Predicting the service-life of adhesively-bonded joints. Int J Fract 2000;103:41-69
14. Aglan H, Abdo Z. An innovative approach to fatigue disbond propagation in adhesive joints. J Adhes Sci Technol 1996;10:183-98
15. Guo Y, Ogin SL, Capell TF, Thorne AM, Reed GT, Wang Y, Tjin SC. Effect of disbond propagation on the reflected spectra of CFBG sensors embedded within the bondline of composite bonded joints. Adv Mater Res 2009;79-82:2067-070
16. De Barros S, Kenedi P, Ferreira S, Bernardino A and Souza L. Influence of mechanical surface treatment on fatigue life of bonded joints. J Adhes 2017;93 (8):599-612
17. da Silva LFM, Ferreira NMAJ, Richter-Trummer V, Marques EAS. Effect of grooves on the strength of adhesively bonded joints. Int J Adhes Adhes 2010;30 (8):735-43
18. Sargent J. Adherend surface morphology and its influence on the peel strength of adhesive joints bonded with modified phenolic and epoxy structural adhesives. Int J Adhes Adhes 1994;14 (1)21-30

19. Shahid M, Hashim S. Effect of surface roughness on the strength of cleavage joints. Int J Adhes Adhes 2002;22 (3):235-44

20. Critchlow G, Brewis D. Influence of surface macroroughness on the durability of epoxide-aluminium joints. Int J Adhes Adhes 1995;15 (3)173-76

21. Kim WS, Yun IH, Lee JJ, Jung HT. Evaluation of mechanical interlock effect on adhesion strength of polymer-metal interfaces using micro-patterned surface topography. Int J Adhes Adhes 2010;30 (6):408-17

22. Jennings C. Surface roughness and bond strength of adhesives. J Adhes 1972;4 (1):25-38

23. Evans J, Packam D. Adhesion of polyethylene to metals: the role of surface topography. J Adhes 1979;10 (3):177-91

24. Zuo Y, Wang H, Zhao J, Xiong J. The effects of some anions on metastable pitting of 3161 stainless steel. Corros Sci 2002;44 (1):13-24

25. Reina JMA, Prieto JJN, Garcìa CA. Influence of the surface finish on the shear strength of structural adhesive joints and application criteria in manufacturing processes. J Adhes 2009;85:324-40

26. Harris A, Beevers A. The effects of grit-blasting on surface properties for adhesion. Int J Adhes Adhes 1999;19 (6):445-52

27. Boutar Y, Naimi S, Mezlini S, Ali MBS. Effect of surface treatment on the shear strength of aluminium adhesive single-lap joints for automotive applications. Int J Adhes Adhes 2016;67:38-43

28. Azari S, Papini M, Spelt J. Effect of surface roughness on the performance of adhesive joints under static and cyclic loading. J Adhes 2010;86 (7):599-612

29. Pereira AM, Ferreira JM, Antunes FV, Bàrtolo PJ. Study on the fatigue strength of AA 6082-T6 adhesive lap joints. Int J Adhes Adhes 2009;29 (6):633-38

30. Bland DJ, Kinloch AJ, Stolojan V, Watts JF. Failure mechanisms in adhesively bonded aluminium: an XPS and PEELS study. Surf Interface Anal 2008;40 (3-4):128-31

31. Alfano M, Lubineau G, Furgiuele F, Paulino GH. Study on the role of laser surface irradiation on damage and decohesion of Al/epoxy joints. Int J Adhes Adhes 2012;39:33-41

32. Galantucci LM, Gravina A, Chita G, Cinquepalmi M. Surface treatment for adhesive-bonded joints by excimer laser. Comp Part A 1996;27 (11):1041-049

33. Wu Y, Lin J, Carlson BE, Lu P, Balogh MP, Irish NP, Mei Y. Effect of laser ablation surface treatment on performance of adhesive-bonded aluminum alloys. Surf Coat Tech 2016;304:340-47

34. Rechner R, Jansen I, Beyer E. Influence on the strength and ageing resistance of aluminium joints by laser pre-treatment and surface modification. Int J Adhes Adhes 2010;30:595-601

35. Musiari F, Moroni F, Favi C, Pirondi A. Durability assessment of laser treated aluminium bonded joints. Int J Adhes Adhes 2019;93:64-75

36. Moroni F, Musiari F, Romoli L, Pirondi A. Influence of laser treatment parameters on the mode I strain energy release rate of aluminium double cantilever beam joints. Int J Adhes Adhes 2018;83:31-40

37. Moroni F. Fatigue behaviour of hybrid clinch-bonded and self-piercing rivet bonded joints. J Adhes 2019;95:577-94

38. Smith EH. Mechanical Engineer's reference book. Butterworth-Heinemann; 1998

39. Slatineau L, Potarniche L, Coteata M, Grigoras I, Gherman L, Negoescu F. Surface roughness at aluminium parts sand blasting. Proc Manuf Syst 2011;6 (2):69-74

40. Romoli L, Moroni F, Khan M. A study on the influence of surface laser texturing on the adhesive strength of bonded joints in aluminium alloys. CIRP Annals 2017;66 (1):237-40